2025 IEEE/SICE International Symposium on System Integration (SII)
January 21-24, 2025, Munich, Germany

Stepping Ahead with Electrified, Connected and Automated Shuttles in the Test Area Autonomous Driving BW

Sven Ochs, Daniel Grimm, Jens Doll, Marc Heinrich, Stefan Orf, Tobias Fleck, Dennis Nienhüser, Miriam Nienhüser, Artur Koch, Thomas Schamm, Ralf Kohlhaas, Steffen Knoop, Peter Biber, Dirk Fratzke, Jakob Kammerer, Ravi Shekhar Jethani, Christian Dewein, Florian Kuhnt, Philip Schörner, Marc René Zofka, Alexander Viehl, J. Marius Zöllner

***Abstract*— Traditional automated shuttle buses plan their trajectories along a fixed path known as virtual rail. Avoiding obstacles on the road, e.g., parked vehicles, imposes challenges on such systems and requires a safety operator to be an active part of the Highly Automated Driving Function (HAD) to maneuver the shuttle around obstacles. In the context of the "EVA Shuttle" project (EVA) we present our developed HAD that is breaking free from the virtual rail. Due to this and the absence of a steering wheel inside the shuttle, a new safety concept had to be developed. We evaluated our approach in the form of a public transport service that bridged the first and last mile using our shuttles in a suburban district in Karlsruhe, Germany.**

I. Introduction

The overarching objective in public transportation is to enhance the overall effectiveness and appeal of the entire system. Consequently, a critical aspect involves advancing innovative mobility ideas that address the first and last-mile challenges. Bridging the final gap in public transport can be achieved by employing electric minibusses that operate autonomously, shuttling passengers between their doorstep and the initial public transport node.

Current approaches rely on fixed virtual rails, which result in halted autonomous shuttles in the presence of obstacles, like parked vehicles alongside the road. The standard solution requires manual interventions or remote operations to drive around these obstacles. During the EVA project, we eliminate the need for virtual rails, granting shuttles the freedom to choose their movement within the boundaries of the road. Therefore, our HAD function has to be capable of sensing, planning, and acting accordingly so that the EVA-Shuttle can solve problems on its own. Since we pioneer dynamic trajectories on public roads, a new safety concept was developed, considering the target speed of 20 km/h. Additionally, to increase the capacity utilization and, therefore, efficiency of the shuttles, an on-demand service is established during the public testing phase, including additional constraints on the mission and routing management.

Achieving our ambitious goals required advancements in safety and the integration of state-of-the-art algorithms and methods. Therefore, a comprehensive concept was developed to combine localization, perception, mission management, planning, and execution into a cohesive system. By integrating these key components, we aimed to create a robust and efficient system capable of meeting our objectives.

Fig. 1: The EVA shuttles Ella, Vera, and Anna have been deployed in a peri-urban area of Karlsruhe. The shuttles choose their movement freely between road boundaries and breaking free from the virtual rail. The steering wheel-free shuttles keep the automated distance from sensed obstacles and, if necessary, drive onto the opposite lane.

The overall system is implemented, tested, and evaluated in the Test Area Autonomous Driving Baden-Württemberg (TAF-BW), which enables the usage of a fleet consisting of three automated electric minibusses. The test area provides wide-ranging opportunities, from intelligent infrastructure for connected driving to accessible proving grounds. One of the test areas is Weiherfeld-Dammerstock, a peri-urban region of Karlsruhe in the southwest of Germany. The peri-urban target area presents particular challenges to automated vehicles, as they encounter diverse road users such as cars, cyclists, pedestrians, narrow streets, and changing parking situations. The consortium consisting of Verkehrsbetriebe Karlsruhe GmbH, Robert Bosch GmbH, TÜV SÜD Auto Service GmbH, and ioki GmbH as well as the consortium lead FZI Research Center for Information Technology tackled the challenge of providing peri-urban public transport on the first and last mile in the most challenging environment for automated driving.

This article is structured as follows: Following this motivation, we present the state-of-the-art in automated mobility concepts in Sec. II. In Sec. III, we focus on the overall concept and the technological steps. Sec. IV presents the

979-8-3315-3161-4/25/$31.00 ©2025 IEEE

results of a 3-month operation period in real traffic. Finally, a summary and research questions that will be pursued in the future form a conclusion in Sec. V.

II. Related Work

The research of current automotive manufacturers focuses on SEA level 2+, and an evolutionary approach to development is being pursued. In Germany, based on the new legal framework [1], it is possible to approve level 3 vehicles. The first was Mercedes Benz, which has an S-Class and EQS [2], which can activate the level 3 function on selected routes and weather conditions. BMW [3] also recieved the permission for Level 3 functionality in their 7 series in July 2024. Tesla [4] is one of the best-known pioneers in autonomous driving. All these vehicles have one thing in common: Steering wheel and pedals. Because the EVA shuttles are designed for last-mile, they lack a steering wheel and pedals. To operate these shuttles as part of public transportation under real-world conditions, a permit from the German government is required. Due to this reason a novel safety concept had to be developed and verified.

In the United States, the emphasis is on individual transportation; however, in Europe, there is also significant research being conducted on autonomous people movers, exemplified by the SHOW project [5]. With the participation of over 69 partners from 13 EU countries, the SHOW project aims to advance the transition of urban traffic environments towards complete sustainability through automation, electrification, cooperation, and inclusiveness. [6] The majority of shuttles involved in the project are produced by EasyMile or Navya and are specifically engineered for autonomous operation, lacking steering wheels and equipped with integrated sensor systems. These shuttles operate on a virtual rail and additionally the safety operator has to verify and validate driving maneuvers [7] [8].

In February 2020, the public transportation authority in Monheim, Germany initiated the deployment of an automated transit line [9]. Five EasyMile EZ10 Gen2 vehicles service this route, with an additional three Gen3 vehicles incorporated since 2023. These shuttles seamlessly integrate into Monheim´s public transit system, covering a route spanning 1.7 km with eight designated stops. Due to the current permission, there is always a safety operator on board the shuttles.

The consortium of the @CITY [10] project investigated multiple challenging scenarios regarding autonomous driving functions. The scenarios include bottlenecks like driving through roundabouts, intersections, or interaction with vulnerable road users. The project results were presented in a controlled environment at the Aldenhoven Testing Center. In contrast to the EVA-Shuttle project were, the shuttles were tested, and the software integrated on a controlled area but later deployed on public roads. This presents numerous challenges due to the unpredictable behavior of other road users, the presence of parked vehicles, and changing conditions from example construction sites.

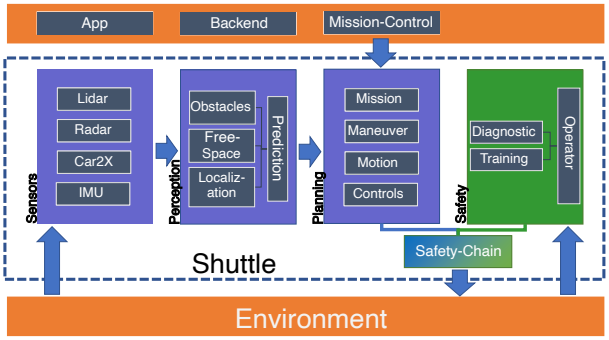

Fig. 2: The architecture follows the sense-plan-act principle (blue pillars). The sensors (left blue pillar), the perception (middle blue pillar), and the planning process (right blue pillar) form the automated driving function. The mission backend communicates with the EVA shuttles. The safety operator inside the shuttle (green pillar) monitors the shuttle's behavior to comply with the safety concept.

Also, at the Aldenhoven Testing Center, the four modular vehicles built up during the UNICARagil [11] project were presented in mid-2023. The autoSHUTTLE is the concept vehicle for future ÖPNV, the Robo-Taxi autoTAXI, the family vehicle autoELF, and the autoCARGO for last-mile transportation. Besides building a common base platform for all four concept vehicles, together with an E/E architecture, the project concentrates on the automation software. Moreover, a particular focus lies on the concept of modular safety. The idea of the UNICARagil project also includes teleoperation with direct control and trajectory guidance [12].

III. Concept

In the following section, the concept of the EVA project will be presented to tackle the previously described challenges. First, Fig. 2 gives an overview of the system architecture.

As the heart of the system, the architecture follows the concept of "sense-plan-act". The sensing part of the environment comprises an inertial measurement unit (IMU), lidar, and radar sensors. The sensors scan the environment and provide data to the downstream perception, which creates a comprehensive environment model. The perception module implemented III-C distinguishes between ground and obstacles, which are further classified as static or dynamic. A novel contribution is the incorporation of point-wise lidar motion estimates into the overall system to avoid false positive motion estimates, e.g. in parked vehicles. Furthermore, a hybrid obstacle detection of learned and engineered features combines the advantages of state-of-the-art detection performance with the ability to detect any object regardless of the training database. The localization, which provides a high-precision global position, completes this module. Using the localization and obstacle information, the prediction module takes over, it forecasts the movements of dynamic road users in the current environment.

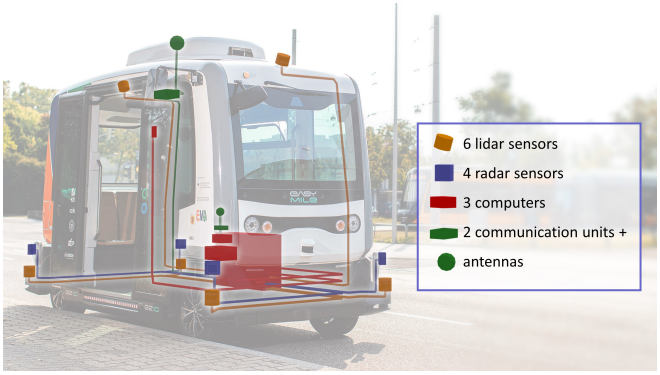

Fig. 3: The base vehicle EasyMile EZ10 Gen2 is equipped with additional components for environment perception, data processing, and communication.

Based on this enhanced environment model, the planning module calculates the shuttle's trajectory. The trajectory has to satisfy the special low-level restrictions of the steering angle, depending on the vehicle's speed. These restrictions are supervised by the control module and executed. These restrictions are one-half of the safety chain. The second half consists of the operator, who monitors the shuttle's behavior from inside the shuttle. The high-level routing and allocation of the shuttles is conducted by the mission control module. This module consists of the passenger app, which collects ride requests. The second is to compare new demands with the state of the fleet and identify the most suitable vehicle to execute the task. The third task is to communicate the routing plan to the assigned vehicle. Communication with intelligent infrastructure can also be integrated through ITS-5G standards within the perception module. The findings from this work will be further developed in the Shuttle2X research project.

A. Vehicle Buildup

The base vehicle of the EVA shuttle is an EZ10 Gen2 vehicle from EasyMile. To cope with the challenges of automated driving in urban environments, an advanced shuttle hardware concept has been developed. Fig. 3 shows the additional hardware components of the EVA shuttles for perception, data processing and communication tasks. Sensing the environment takes place at each corner of the vehicle by multilayer 360-degree lidar and radar sensors. Two additional lidar sensors are placed on the roof of the vehicle. Data acquisition and processing occur on three different computers, which are installed in the shuttles. Each computer is responsible for a different part of the automated driving software. The perception computer provides raw sensor data, an environment model, and a CAN interface to the shuttle's internal control units. An additional dedicated computer is in charge of motion planning as well as Human Machine Interface (HMI). The third computer is used to handle communication with the mission backend. To support the increased power consumption of the additional hardware components, a high-capacity power supply is installed that makes use of the electric energy of the main batteries of the vehicle.

B. Mission Management

All EVA shuttles are run in a demand-driven mode, which implies there are neither fixed routes nor any fixed timetables. The inevitable consequence is the base requirement to be able to change the destination (mission goal) dynamically. The core responsibilities of the on-demand operating system can be divided into two components: Matching an incoming request to a vehicle and generating a mission for execution.

1) On-demand Operating System for Digital Mobility: To record the mobility demand of users, smartphone apps for iOS and Android were developed and published in the respective stores. The app scored 4.6 out of 5 stars from an overall 1.290 downloads in the respective app stores.

The receiving servers of the on-demand operating system process the ride requests. The goal is to find a vehicle in the fleet that can add the new request to its current plans. On the other hand, accepting the request should not increase the duration for passengers already in the vehicle. Additionally, the restrictions regarding possible maneuvers, driving speeds, and even permissions to drive on certain streets must be considered. Because of this reason, special routing algorithms had to be created that respect these limitations and any restrictions from the allowed set of routes. Eventually, a shared mission format for the Operational Design Domain (ODD)-specific routes will be exposed to the driving stack.

2) Mission Execution: The goal of the on-demand service is to keep vehicle routes as dynamic as possible without interfering with the planning algorithm in critical scenarios such as intersections. To cope with this issue, a route is broken up into segments. These segments are continuous and have no overlap. Due to this reason, the mission backend releases the subsequent segment to the planning algorithm, if the vehicle comes close to the end of the last segment. Deployed segments are neither cancellable nor changeable to provide a constant corridor for the motion planning algorithms.

C. Perception

The perception of the EVA shuttles consists of the localization and the environment model, including obstacle detection.

1) Localization: For the described application scenario, a highly precise and reliable estimate of the vehicle pose is necessary. Simply using consumer GNSS for localization unfortunately is not sufficient, in particular in urban scenarios where occlusions by buildings will likely introduce errors or continuous drift in position estimation. The EVA shuttles therefore use a lidar based simultaneous localization and mapping (SLAM) approach for localization.

Besides *simultaneous* localization and mapping, the utilized SLAM system may as well be used in a dedicated localization-only mode. The applied solution in the work at hand was therefore split into a two-stage approach with different sensor setups. Initially, a mapping run was performed to record odometry, IMU, lidar and GNSS data

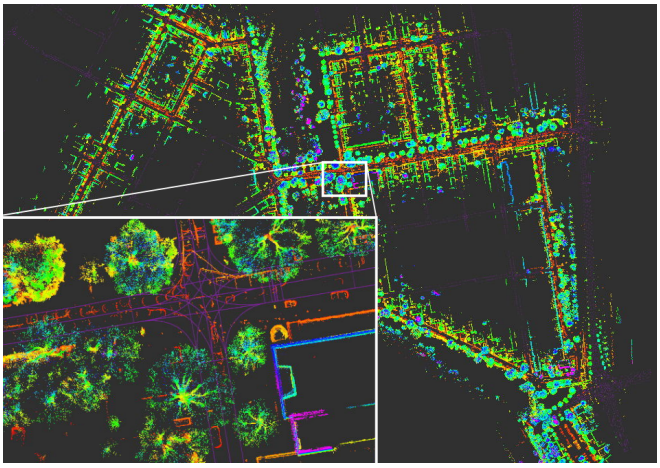

Fig. 4: SLAM map for the Weiherfeld-Dammerstock test site. Overlay of semantic map elements (purple) and pointcloud map obtained from SLAM. The Color encodes different point height values.

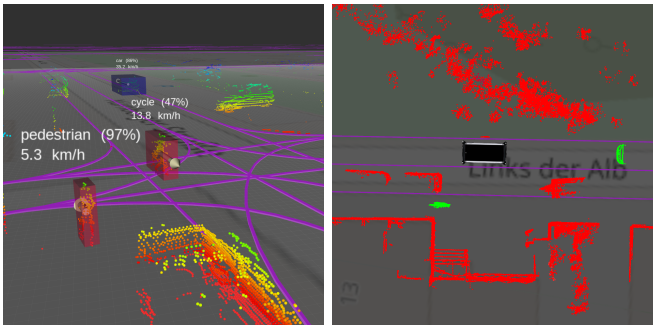

(a) Object detecion with labels (b) Static and moving lidar points

Fig. 5: 5a shows moving objects by Lidar object detection with classification and velocity information. 5b presents Lidar motion segmentation results for a scene with two moving objects. The red color denotes lidar points detected as stationary, and green ones are detected as moving. Map underlay © OpenStreetMap.

while covering the complete target area. Recorded data was employed to generate maps offline, offering the potential for retrospective optimization of involved hyperparameters.

Figure 4 depicts the resulting SLAM map used during localization. The map contains points of vertical structures and poles extracted from input point clouds obtained from two 3D lidar sensors mounted on top of the vehicle. These features have proven to be sufficient w.r.t. precision and robustness in the urban target environment. Odometry and IMU data were additionally used for scan-leveling and to remove distortion artifacts caused by ego-motion. The overlay in the figure additionally shows both the semantic and the localization map. The required geo-referencing of the semantic map (mainly used for planning) was achieved by using additional GNSS anchors during the mapping stage. As can be seen, dynamic objects appear as artifacts inside the SLAM map and therefore are automatically removed in a post-processing step prior to final map deployment.

After successful map creation, the resulting map is used online for localization in all three shuttles with adapted extrinsic parameters for the equipped sensors. Opposed to the mapping stage, localization does not rely on GNSS observations. Instead map matches based on the Normal Distributions Transform [13] are used to correct accumulated drift from lidar odometry. The same SLAM system placed second in the HILTI SLAM challenge 2021 [14] with a mean absolute error of 7.6 cm.

Localization may be initialized manually by the operator from a set of pre-defined localization positions that are annotated in the semantic map. This initial guess is then further refined in a Monte-Carlo fashion using local optimization through randomized map-matching in a small radius around the starting pose until sufficient convergence is achieved within the provided SLAM map.

2) Environmental-model: The environment model provides two data structures for path planning: An object list for dynamic objects and an occupancy grid for both stationary and moving objects.

The object list includes motion tracking properties and object type classification for short-term position prediction of dynamic objects. It originates from a track-level fusion of object lists generated by the sensor modalities radar and lidar. While radar object detection focuses on moving vehicles using a radar vehicle reflection model and multiple Kalman filters, lidar object detection attaches properties to each lidar point: ground vs. object ID [15], motion (cf. Fig. 5b) [16] and object type classification using an SVM-based classification. Similar to radar object detection, multiple Kalman filters track the objects detected in each sensor measurement cycle. An exemplary visualization of the object list is depicted in Fig. 5a. In order to improve performance for vehicle detection in lidar data further, a PIXOR-like deep learning approach [17] is executed in parallel. Its results are used to refine object IDs to avoid over-segmentation problems for vehicles and increase the detection range, as in [15]. Hence, the hybrid approach combining [15] and [17] improves detection results for vehicles, while keeping the ability to detect moving objects of arbitrary shape that may have never appeared in a training database.

Finally, the occupancy grid provides a consistent view of the lidar object detection results in a grid structure. Both stationary and moving objects are included. Cell properties allow filtering the information such that generating e.g. an occupancy grid of only stationary objects becomes a simple post-processing step.

D. Planning

The goal of the planning module is to provide feasible and safe behaviors and trajectories while leveraging the available space. Our approach contrasts with typical approaches that follow fixed paths. The planning pipeline is divided into three parts: a mission module, maneuver decision, and geometric planning.

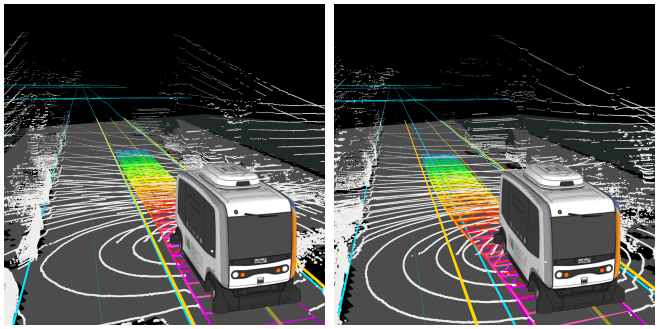

(a) Before expanding to the opposite lane.

(b) After expanding to the opposite lane.

Fig. 6: Visualization of the planning algorithm. The rainbow colors denote the point in time of each trajectory pose, color-coded from purple over yellow to blue. The lateral constraints of the maneuver planner are shown in yellow. The cyan lines show the lane information of the high-definition lanelet map.

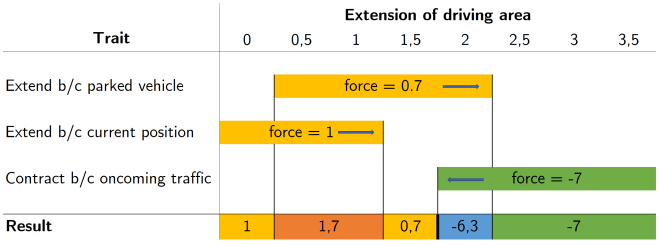

Fig. 7: Visualization of the resolving process for incoming announcements of the maneuver module. In the first step, all intervals are intersected, and the forces are added. The second step includes the search for the equilibrium of the forces. In the presented case, the green interval enforces a maximum extension of the driving area. The other traits vote for an extension. The consent is found by searching for the sign change.

1) Mission: The mission module handles the challenge of always providing a valid drivable corridor to the rest of the planning pipeline. As already established in Section III-B.2, the overall mission is fed to the mission module segment-wise. The segments are large enough to guarantee a valid trajectory, usually till the next intersection. The mission module calculates a detailed route on lane level from these segments, using the high-definition map in lanelet2 [18] format. From this route, a driveable corridor called a driving area is created, shown as yellow lines in Fig. 6. Subsequently, the driving area can be adjusted via the maneuver module to align with the prevailing situation.

2) Maneuver: The maneuver module uses a consensus-based decision-making process to handle complex situations. A complex scenario is broken down into micro-decisions, where each decision addresses another behavior aspect. Currently, maneuver decisions are divided into five domains: driving area extension, lateral offset, desired speed, stop lines, and indicators. Each decision within a domain is handled by so-called traits, which represent a certain behavior within the overall maneuver. The traits provide an interval for the different domains with an upper or lower bound or both. All votes are collected by the controller and then resolved via the consensus-based approach. For modeling a hierarchy inside a complex situation, each trait is attributed with a weight, so-called force.

To showcase the functionality of our maneuver module, which remains consistent across all aspects, we have chosen a typical scenario for illustrative purposes. This scenario involves parked vehicles obstructing sections of our lane, as depicted in Fig.6. When additional space beyond our lane is required, we extend our driving area into the opposing lane. The extensions are exemplary and represented by two traits, depicted as rows. To inhibit an extension in the case of oncoming traffic, a contracting trait will overrule the other traits. As a consequence, this trait has a higher force with an opposite sign as the extension traits. The resolution of the incoming announcements is presented in the result row at the bottom of Fig. 7. Initially, intervals are pairwise intersected to create disjoint intervals, followed by the summation of forces within these disjoint intervals. Finally, the consensus is achieved by conducting a linear search for sign changes within the disjoint intervals, indicating the equilibrium of influencing forces. In the presented scenario, applying a linear search yields the identification of a blue box, correlating with an expansion of the driving space by 2 meters. These constraints are passed down to the motion planning process for further processing.

3) Motion: The motion planning calculates a geometric trajectory given the constraints. Besides vehicle kinematics and dynamics, those constraints include the environment model with its obstacles, the maneuver decisions, and the driving corridor. Moreover, the planning algorithm seeks to optimize for driving comfort and progress. The planner plans a trajectory of N discrete poses with constant time intervals. Constraints can be divided into external and internal constraints. The former are determined by collisions with obstacles and the boundaries of the driving area corridor. Here, the safety concept from Sec. III-E is applied and checked for violations against the contours of the predicted obstacles. The boundary conditions implied by the maneuver decision are represented as lateral and longitudinal limitations of the driveable area over time. Internal constraints consider the dynamic and kinematic characteristics of the vehicle. These are modeled as longitudinal and lateral acceleration limits, steering rates, and curvature constraints.

Optimal trajectories are determined using a non-linear optimizer based on Particle Swarm Optimization [19], a meta-heuristic optimization algorithm inspired by the flocking behavior of fish or birds. Each particle represents a trajectory candidate. Generating initial trajectory candidates relies on heuristics comprising the course of the road and the previous planning result. During optimization, a cost function comprising efficiency, comfort, and safety aspects is minimized. Minimizing accelerations and yaw rates or

higher derivatives achieves comfortable and smooth trajectories. Furthermore, deviations from the reference speed are punished, especially exceeding the reference speed. To obtain a high level of safety, distances to obstacles and lane boundaries are maximized. The optimization process can handle discontinuous functions like the safety margins obtained by the safety concept III-E. A visualization of the planned trajectory is shown in Fig. 6. The complete trajectory planner can be found in [20] and the specialized version in [21].

E. Safety

The ambitious goals of the EVA project, namely allowing the software to perform free driving decisions and to increase the permitted maximum speed to 20 km/h, while having no steering wheel for a safety operator to take over, required a novel safety concept.

We had to guarantee a safe operation for mandatory permission on German public roads according to ISO26262 [22]. This posed a challenge because the EasyMile EZ10 Gen2 vehicles used in the project have neither a steering wheel nor pedals. Since the safety operator, always on board, can not control the vehicle while moving autonomously, safety has to be assured differently. For this purpose, a Hazard Analysis and Risk Assessment (HARA) was performed, analyzing the shuttle, software, and safety operator inside the shuttle. The goal of the HARA is to detect potential malfunctions that could lead to hazards, e.g., accidents, and assess them by exposure, severity, and controllability. During this process, all possible impediments to automation were linked to traffic situations and accident scenarios. All combinations were analyzed, and a safety goal and a safe state were derived. As a result, we set the following constraints to the ODD:

- No driving at night due to poor visibility
- No driving on ice or snow due to longer braking distances
- Only driving on roads with a maximum speed limit of 30 km/h due to high severity in case of an accident
- Safety operator needs to track lateral and longitudinal distances to objects

To fulfill the last mentioned point, we introduce the concept of a dynamic safety cell, a precisely defined area around the vehicle, which needs to be free of obstacles at any time so that a potential malfunction of the AD function can be detected by the safety operator and a collision-free emergency break can be engaged. The spatial dimensions of the cell are derived from the reaction time of the safety operator and the vehicle's braking. To determine the cell's width, we injected the malfunction unintended steering, waited for 0.6 s, equivalent to the reaction time of the safety operator, and engaged the emergency brakes. Precise measurements were acquired utilizing high-precision GNSS. A sequence of trials was conducted on a proving ground, with velocities incrementing by 2.5 km/h. The orange dots in Fig. 8 show the measured lateral offset. The safety cell is segmented into velocity intervals to compensate for the inherent limitations in humans' ability to gauge the vehicle's current speed accurately. The blue bars show the chosen velocity intervals and lateral cell expansions. The same process is repeated for the longitudinal size of the cell. The sizes for 5 km/h, 12.5 km/h and 20 km/h are 2.1 m, 6.2 m and 15 m. The cells are sized conservatively, implementing a "safety first" paradigm. Thus, even in an error case, enough space persists between obstacles and every possible shuttle trajectory for the operator to intervene.

As of 2023, new regulations in Germany, as mandated by [23], permit the authorization of SAE Level 4 vehicles. Although this regulation was not in effect during the project period, the discoveries and safety concepts developed can be applied under the new legislation.

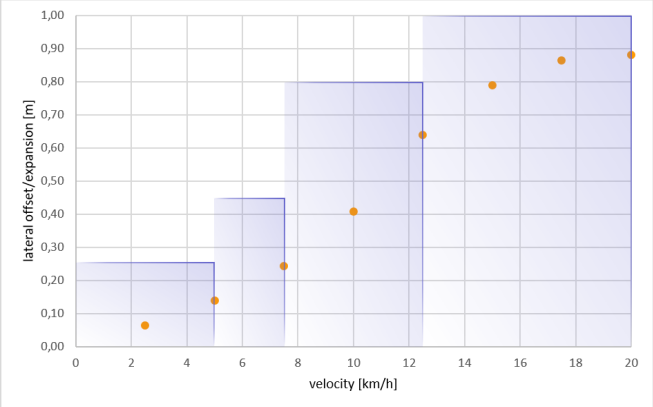

Fig. 8: Measures of the safety cell – Mean lateral offset for unintended steering (orange) and lateral expansion of the resulting safety cell (blue areas) for different vehicle velocities.

1) Health Monitoring and User-Interface: The employed safety operators, in general, did not have a technical background, nor did they participate in the preceding engineering process. The main interaction component with the shuttle is a touch screen user interface. It's main purpose is to display the AD software's status information like the vehicle's current health state, including state of charge and odometer.

The health module follows an observer-based approach for monitoring system properties of the component-based architecture [24]. Responsiveness and self-states of individual components and message rates of communication paths are monitored to derive health information about the system's parts. With predefined limits, an abstracted system property's health state

$$S_p \in \{0 = OK, 1 = WARNING, 2 = ERROR\} \quad (1)$$

is generated. E.g., for the localization component (denoted l), the rate of the calculated vehicle's pose is analyzed and translated into its system property health state $S_p^{(l)}$ by using thresholds. Similarly, responsiveness and self-states (e.g., from perception drivers) are also considered. The individual interoceptive health states are collected and aggregated into a health tree, mapping the system's parts. Each node represents

TABLE I: Overview of booking stats by week.

	22.04.21 - 25.04.21	26.04.21 - 02.05.21	03.05.21 - 09.05.21	10.05.21 - 16.05.21	17.05.21 - 23.05.21	24.05.21 - 30.05.21	31.05.21 - 06.06.21	07.06.21 - 13.06.21	14.06.21 - 20.06.21	21.06.21 - 27.06.21	28.06.21 - 04.07.21	05.07.21 - 11.07.21
no offer	1206	1093	604	462	182	663	343	74	46	156	91	85
no booking	259	229	216	184	72	98	143	120	102	136	82	74
Cancelled booking	22	13	46	47	21	27	43	34	27	45	29	26
ride	53	68	76	101	33	33	76	60	60	89	37	69
sum	1540	1403	942	794	308	821	605	288	235	426	239	254
offer ratio	22 %	22 %	26 %	42 %	41 %	19 %	43 %	74 %	80 %	63 %	62 %	67 %
ride ratio	3 %	5 %	8 %	13 %	11 %	4 %	13 %	21 %	26 %	21 %	15 %	27 %

aggregated system parts (e.g., localization, perception, planning) in different levels of granularity. Because of the tightly coupled system, failures often propagate through multiple components. As a result, an error manifests in multiple erroneous health states, making identifying the root cause almost impossible. Therefore, such dependencies between health states are also modeled. The generation of a single output health state $S_c^{(x)}$ for component x, with it's system property health state $S_p^{(x)}$ and dependent states $S_c^{(d_1)}, \ldots, S_c^{(d_n)}$ is then:

$$S_c^{(x)} = \begin{cases} S_p^{(x)}, & \max(S_c^{(d_1)}, \ldots, S_c^{(d_n)}) = 0 \\ 0, & \max(S_c^{(d_1)}, \ldots, S_c^{(d_n)}) \neq 0. \end{cases} \quad (2)$$

As a result, the health monitoring module focuses on the true cause of malfunctions. A dedicated screen shows the aggregated health states of the system's parts to the safety operator. This information helps the safety operator understand the current error and aids a remote operator or developer in giving purposeful support. Furthermore, the health state information is used to disengage the autonomous driving software from the vehicle, in which case the vehicle enters a minimum risk state by deceleration.

IV. Results

The on-demand test operation with passengers proved to be a success. We received more than 8.000 trip requests via our EVA app, where the shuttles were able to complete 750 trips. Table I shows that the gap between the number of requests and trips originates mainly from the first months of the test operation. This can be explained due to extensive advertising in the local press and social media initially. Overall, 68% of the trips started or ended at the tram station on Weiherfeld-Dammerstock. To increase the number of trips, the average velocity of the shuttles should be further increased. This was also a result a the survey since 72% of the passenger and participants wished for a higher speed. A high velocity of up to 20 km/h could be achieved while driving on the main roads. The challenging parts were mostly narrow roads, where the shuttle reduced its velocity because of the safety-cell size and tight corners.

During the passenger operation, a survey was conducted regarding different aspects such as user acceptance and driving performance. In general, the users felt safe and attributed the automated shuttles to a bright future in public transportation. An excerpt of the results of the survey is listed below:

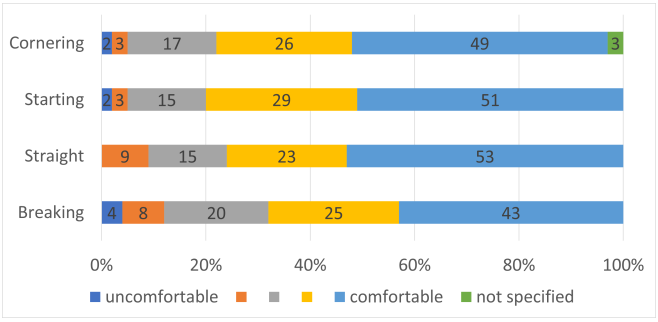

Fig. 9: A survey was conducted regarding the driving behavior. Across all topics, cornering, straight, starting and braking, approximately half of the participants felt comfortable.

- 93 % of the participants would use the EVA shuttles again
- 93 % of the participants felt safe during the ride
- 89 % of the participants felt comfortable during the ride
- 73 % of the participants believe that projects like EVA will improve the traffic situation
- 61 % of the participants believe that project like EVA will improve the safety

Another aspect focused mainly on the driving behavior of the EVA shuttles. Across all topics, cornering, straight, starting, and braking, approximately half of the participants felt comfortable, as seen in Fig. 9.

Table II shows the mileage of each shuttle during the last test phase. Two shuttles were used for the on-demand operation. The third was used for development runs, testing optimizations, and experimental features. Due to this fact, Vera and Anna got a low mileage in the first month when they were used on KIT-Campus Ost and also in Weiherfeld-Dammerstock. Overall the EVA shuttles drove over 3.500 km including software integration tests and permission purposes. With 1.746 km Ella drove the most kilometers, followed by Vera with 1.039 km and Anna with 778 km. During regular daily operations, primarily between 8 AM and 5 PM, a range of conditions were encountered, including varying weather, rush-hour traffic, and the end of the school day when many cyclists were present.

TABLE II: Mileage of each EVA shuttle during passenger transport.

	mileage [km]				
Shuttle	April	May	June	July	Grand Total
Ella	281	784	264	51	1.380
Vera	55	139	414	407	1.015
Anna	-	117	527	43	687
Total	336	1040	1205	501	3082

V. Conclusion

In the EVA project, we stepped ahead with a new on-demand concept for automated shuttles on the first and last mile in public transport. This concept includes a user-friendly user interface, an on-demand service with ride-pooling. State-of-the-art algorithms were adapted and tailored specifically for the needs of the EVA project. Dynamic rerouting capabilities were introduced for last-minute bookings to minimize passenger wait times. A significant advancement in integrating autonomous shuttles into mixed traffic flow is the implementation of dynamic planning. This enhancement relies on several critical factors, including high-precision localization, accurate identification of both static and dynamic obstacles, and comprehensive maneuver planning that integrates all available data. This allows us to let the EVA shuttles drive around static obstacles and break free from the virtual rail. This also includes maneuvering into the oncoming lane if stationary obstacles obstruct the vehicle's own lane. This is key to coping with tight suburban streets with parked vehicles alongside the street and also reduces the interventions of the safety operator. Increasing the maximum speed to 20 km/h lets the shuttles keep up with surrounding traffic and necessitated the development of a new safety concept. We proved this concept by implementing real passenger transport for three months with 1000 users in 700 trips. Non-specialist safety operators were able to supervise the vehicles following a novel safety concept that speaks for the overall concept.

Acknowledgment

This research was partially supported by the German Federal Ministry for Digital and Transport (BMDV) in the funding program Automated and connected driving under the project EVA-Shuttle-Busse (16AVF2117A).

This research was partially supported by the German Federal Ministry for Economic Affairs and Climate Action (BMWK) in the funding program New vehicle and system technologies under the project Shuttle2X (19S22001B).

References

[1] "Straßenverkehrsgesetz (stvg) § 1a kraftfahrzeuge mit hoch- oder vollautomatisierter fahrfunktion," https://www.gesetze-im-internet.de/stvg/__1a.html, accessed: 2024-03-26.

[2] "Mercedes group: Autonomes fahren," https://group.mercedes-benz.com/innovation/produktinnovation/autonomes-fahren/, accessed: 2024-03-26.

[3] "Hochautomatisiertes fahren auf level 3 im neuen bmw 7er," https://www.press.bmwgroup.com/deutschland/article/detail/T0438214DE/ab-fruehjahr:-hochautomatisiertes-fahren-auf-level-3-im-neuen-bmw-7er?language=de, accessed: 2024-08-09.

[4] "Tesla Autopilot sensor-setup and autonomous driving software," https://www.tesla.com/autopilot, accessed: 2021-10-26.

[5] "SHOW shared automation operating models for worldwide adoption," https://show-project.eu/, accessed: 2021-10-26.

[6] Y.-P. Flötteröd, L. Bieker-Walz, and J. Olstam, "Towards safe and efficient shared-space oriented drt service: someinsights with real case study in linköping," in *ITS World Congress 2021, 11.-15. Okt. 2021, Hamburg, Germany.*, 2021.

[7] I. Erdelean, A. Schaub, C. Stefan, M. Vanžura, V. Praendl-Zika, and A. Hula, "Assessment of physical road infrastructure to support automated vehicles in an urban environment," *Transportation research procedia*, vol. 72, pp. 2385–2392, 2023.

[8] A. Anund, R. Ludovic, B. Caroleo, H. Hardestam, A. Dahlman, I. Skogsmo, M. Nicaise, and M. Arnone, "Lessons learned from setting up a demonstration site with autonomous shuttle operation–based on experience from three cities in europe," *Journal of Urban Mobility*, vol. 2, p. 100021, 2022.

[9] "Bahnen monheim: die altstadtstromer," https://www.bahnen-monheim.de/autonomer-bus/ziele-und-motivation, accessed: 2024-03-26.

[10] "@city: Automated driving in the city," https://www.atcity-online.de/, accessed: 2024-03-26.

[11] L. Eckstein and S. Pischinger, Eds., *29. Aachen Colloquium Sustainable Mobility : October 5th-7th, 2020, digital event, 1-2; 1. Edition*. [Online]. Available: https://publications.rwth-aachen.de/record/814885

[12] T. Homolla and H. Winner, "Encapsulated trajectory tracking control for autonomous vehicles," *Automotive and Engine Technology*, vol. 7, no. 3, pp. 295–306, 2022.

[13] P. Biber and W. Straßer, "The normal distributions transform: A new approach to laser scan matching," in *Proceedings 2003 IEEE/RSJ International Conference on Intelligent Robots and Systems (IROS 2003)(Cat. No. 03CH37453)*, vol. 3. IEEE, 2003, pp. 2743–2748.

[14] M. Helmberger, K. Morin, B. Berner, N. Kumar, G. Cioffi, and D. Scaramuzza, "The hilti SLAM challenge dataset," *IEEE Robotics and Automation Letters*, vol. 7, no. 3, pp. 7518–7525, jul 2022. [Online]. Available: https://doi.org/10.1109%2Flra.2022.3183759

[15] F. Moosmann, *Interlacing self-localization, moving object tracking and mapping for 3d range sensors*. KIT Scientific Publishing, 2013, vol. 24.

[16] K. Jo, S. Lee, C. Kim, and M. Sunwoo, "Rapid motion segmentation of lidar point cloud based on a combination of probabilistic and evidential approaches for intelligent vehicles," *Sensors*, vol. 19, no. 19, p. 4116, 2019.

[17] B. Yang, W. Luo, and R. Urtasun, "Pixor: Real-time 3d object detection from point clouds," in *Proceedings of the IEEE conference on Computer Vision and Pattern Recognition*, 2018, pp. 7652–7660.

[18] F. Poggenhans, J.-H. Pauls, J. Janosovits, S. Orf, M. Naumann, F. Kuhnt, and M. Mayr, "Lanelet2: A high-definition map framework for the future of automated driving," in *21st International Conference on Intelligent Transportation Systems (ITSC)*. IEEE, 2018.

[19] R. Eberhart and J. Kennedy, "Particle swarm optimization," in *Proceedings of the IEEE international conference on neural networks*, vol. 4. Citeseer, 1995, pp. 1942–1948.

[20] S. Ochs, J. Doll, M. Heinrich, P. Schörner, S. Klemm, M. R. Zofka, and J. M. Zöllner, "Leveraging swarm intelligence to drive autonomously: A particle swarm optimization based approach to motion planning," 2024.

[21] P. Schörner, M. T. Hüneberg, and J. M. Zöllner, "Optimization of sampling-based motion planning in dynamic environments using neural networks," in *2020 IEEE Intelligent Vehicles Symposium (IV)*. IEEE.

[22] "Road vehicles — Functional safety — Part 3: Concept phase," International Organization for Standardization, Geneva, CH, Standard, Dec. 2018.

[23] "Bmdv - germany will be the world leader in autonomous driving," https://bmdv.bund.de/SharedDocs/EN/Articles/DG/act-on-autonomous-driving.html, accessed: 2024-04-08.

[24] S. Orf, S. Ochs, J. Doll, A. Schotschneider, M. Heinrich, M. R. Zofka, and J. M. Zöllner, "Modular fault diagnosis framework for complex autonomous driving systems," 2024. [Online]. Available: https://arxiv.org/abs/2411.09643